

***Final Draft***  
**of the original manuscript:**

Stark, A.; Bartels, A.; Clemens, H.; Kremmer, S.;

Schimansky, F.-P.; Gerling, R.:

**Microstructure and Texture Formation During Near  
Conventional Forging of an Intermetallic Ti-45Al-5Nb Alloy**

In: Advanced Engineering Materials (2009) Wiley

DOI: 10.1002/adem.200900117

**Microstructure and Texture Formation during Near Conventional Forging of an Intermetallic Ti-45Al-5Nb Alloy\*\***

Andreas Stark\*, Arno Bartels, Helmut Clemens, Sascha Kremmer, Frank-Peter Schimansky and Rainer Gerling

*[\*] Dr. A. Bartels, A. Stark, Institute of Materials Science and Technology, Hamburg University of Technology, Eißendorfer Str. 42, D-21073 Hamburg, Germany, E-mail: stark@tu-harburg.de*

*Dr. S. Kremmer, Böhler Schmiedetechnik GmbH&CoKG, Mariazellerstraße 25, A-8605 Kapfenberg, Austria*

*Prof. Dr. H. Clemens, Department of Physical Metallurgy and Materials Testing, Montanuniversität Leoben, Franz-Josef-Straße 18, A-8700 Leoben, Austria*

*Dr. F.-P. Schimansky, Dr. R. Gerling, Institute for Materials Research, GKSS Research Center, Max-Planck-Straße 1, D-21502 Geesthacht, Germany*

*[\*\*] The authors thank Dr. H. F. Chladil for helpful discussions. Part of this work was financially supported by the German Science Foundation, DFG (Projects: BA 1147/1-1, GE 1115/1-1) and the Styrian Materials Cluster.*

Keywords: Intermetallics, titanium aluminides, forging, texture, microstructure

The continuous demand for weight reduction and higher engine efficiencies in aerospace and energy industries pushes the materials applied today towards their limits. Therefore, there is a strong need for developing novel light-weight materials which can withstand temperatures up to 800 °C maintaining reasonable mechanical properties.<sup>[1,2]</sup> Intermetallic  $\gamma$ -TiAl based alloys exhibit numerous attractive properties for high-temperature structural applications in industrial and in aviation gas turbines as well as aerospace and automobile industries.<sup>[3]</sup> In order to extend their service range to higher temperatures research activities have been focused on high Nb bearing TiAl alloys. These so-called 3<sup>rd</sup> generation alloys exhibit a significant increase in strength combined with improved creep properties and oxidation resistance, see references.<sup>[4,5,6]</sup>

However, up to now there is no well established wrought processing route which guarantees an economic and continuous supply of aerospace and stationary turbine components made of  $\gamma$ -TiAl.<sup>[2,7,8,9]</sup> Regarding wrought processing most of the approaches reported in literature include an isothermal forging step.<sup>[9,10]</sup> For example, for the production of aeroengine blades isothermal forging of  $\gamma$ -TiAl is performed at high constant temperatures, requiring special dies and environmental conditions which increase the manufacturing costs. In order to increase the economic feasibility of the wrought processing route for  $\gamma$ -TiAl components a “near conventional” forging of  $\gamma$ -TiAl based alloys using hot dies has been developed.<sup>[11,12]</sup>

As mentioned above, several thermo-mechanical processing routes have been established for conventional  $\gamma$ -TiAl based alloys, such as hot rolling, extrusion and forging.<sup>[3,9]</sup> In this context strong anisotropic mechanical behaviour due to the formation of crystallographic textures is often reported.<sup>[13,14]</sup> Several papers dealing with microstructure evolution, texture analysis and texture formation of the  $\gamma$ -TiAl phase during hot working have

been published in the last years.<sup>[14,15,16,17,18,19]</sup> However, little information is available on the deformation behaviour and texture evolution of the  $\alpha$ -Ti(Al)/ $\alpha_2$ -Ti<sub>3</sub>Al phase at high temperatures.

In this study, microstructure and texture formation in an intermetallic Ti-45Al-5Nb alloy (composition in atomic percent) during near conventional forging on an industrial scale in the ( $\alpha$ + $\gamma$ ) phase region between 1200 °C and close to the  $\alpha$ -transus temperature ( $T_\alpha = 1295$  °C) are investigated. The obtained results are compared with those derived from laboratory uniaxial compression tests conducted within the ( $\alpha_2$ + $\gamma$ ) phase region.<sup>[20]</sup> Hot-isostatically pressed powder compacts were used throughout this study. These compacts show no initial texture and are microstructurally as well as chemically homogeneous. The starting material was thoroughly analysed regarding microstructure and phase transition temperatures.

## Material and Experiment

Specimens with a base composition of Ti-45Al-5Nb were deformed in various forging tests on an industrial scale. In order to start with texture-free and microstructurally as well as chemically homogeneous material hot-isostatically pressed powder compacts were used. The powder was produced in the PIGA-facility (Plasma Melting Induction Guiding Gas Atomization) at the GKSS Research Centre.<sup>[21]</sup> Powder of the size fraction < 180  $\mu\text{m}$  was filled in Ti cans, which then were degassed, welded and subsequently hot-isostatically pressed (HIP) at 200 MPa for 2 h at 1250 °C. Chemical analyses indicated that the composition of both, the alloy powder and the HIPed materials, match the nominal compositions within the experimental error. After HIPing, the content of oxygen and nitrogen was analyzed to be 450 mass-ppm and 50 mass-ppm, respectively. For the forging tests cylindrical specimens (41 mm in diameter and 44 mm in height) were cut from these powder compacts by spark erosion technique.

The industrial forging process used in this study is called “near conventional”, because hot-forging is performed on a conventional 1000 t hydraulic press without any special isothermal forging equipment.<sup>[11]</sup> However, due to the high strain rate sensitivity of  $\gamma$ -TiAl based alloys and thus the necessity of very low deformation speeds it is vital to pre-heat the dies prior to forging to avoid excessive cooling during deformation. The die temperature during forging is approximately 400 °C to 800 °C below the billet temperature. The hydraulic press has been specially automated to provide the possibility to run at low die speeds and to allow an exact control of die speed, position and temperature during the whole process. Prior to forging a heat shielding layer is applied to the Ti-45Al-5Nb specimens to reduce heat loss during transfer from the furnace to the press as well as during the forging process.<sup>[11]</sup> The TiAl billet is heated up to forging temperature in an electric furnace under argon atmosphere. After holding on temperature for a defined time the billet is manually transferred into the press within 5 seconds and the forging process is started. The total contact time between the billet and the dies can last up to 60 seconds depending on die speed and total stroke. The forging tests were conducted at 1200 °C, 1270 °C and close to the  $\alpha$ -transus temperature ( $T_\alpha$ ). The cylindrical specimens were forged to an overall logarithmic strain of approximately 0.7 followed by air cooling.

Microstructure observation was made by light-optical microscopy (LOM) and scanning electron microscopy (SEM) in back-scattered electron (BSE) mode. The volume fractions of the different phases within the samples were estimated by X-ray diffraction (XRD) measurements as well as by quantitative metallographic evaluation conducted on both SEM images taken in BSE mode and LOM images of colour etched samples.

Texture measurements have been performed by XRD in reflection geometry with filtered Cu  $K\alpha$  radiation using a texture goniometer with eulerian cradle and parallel beam optic from Bruker AXS. Pole figures of the  $\gamma$ -TiAl phase and of the  $\alpha_2$ -Ti<sub>3</sub>Al phase were measured up to a pole distance angle ( $\chi$ ) of 85° and subsequently corrected for background

and intensity loss. The orientation distribution function (ODF) of the  $\gamma$ -TiAl phase was calculated by using the series expansion method<sup>[22]</sup> up to an order of 22. The ODF of the  $\alpha$ -Ti(Al)/ $\alpha_2$ -Ti<sub>3</sub>Al phase was calculated employing the WIMV algorithm of the BEARTEX Berkeley Texture Package.<sup>[23]</sup> Subsequently, complete and inverse pole figures were recalculated from the ODF.

## Results and Discussion

### Microstructure and phase composition

The microstructure of HIPed Ti-45Al-5Nb powder compacts is shown in Figure 1. A duplex microstructure is formed due to HIPing in the middle of the ( $\alpha$ + $\gamma$ ) phase field and furnace cooling to room temperature. The grain size is in the range of 10 to 20  $\mu\text{m}$ . The microstructure is very homogeneous and shows no visible segregation. The XRD pattern of the HIPed powder compact shows only peaks of  $\gamma$ -TiAl and  $\alpha_2$ -Ti<sub>3</sub>Al phase and the phase fractions as determined by Rietveld analysis amount to approximately 75 vol.%  $\gamma$ -TiAl and 25 vol.%  $\alpha_2$ -Ti<sub>3</sub>Al. This result is in good agreement with that obtained from quantitative metallographic evaluation conducted on SEM- and LOM-images. The phase transformation temperatures of Ti-45Al-5Nb which are important parameters for the following thermo-mechanical process are determined by differential scanning calorimetry (DSC).<sup>[24]</sup> The eutectoid temperature ( $\alpha_2$ + $\gamma \rightarrow \alpha$ ) is 1151 °C and the  $\alpha$ -transus temperature ( $\gamma \rightarrow \alpha$ ) is 1295 °C.

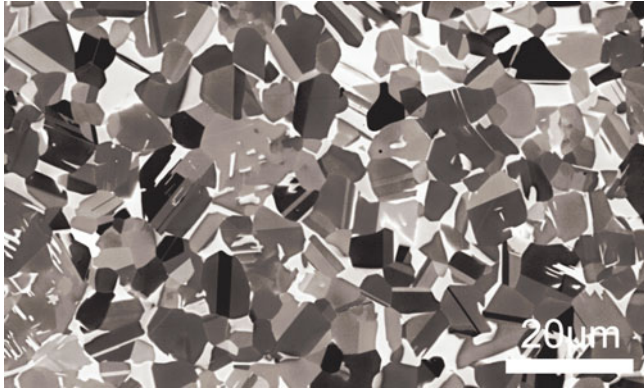


Fig. 1. Microstructure of Ti-45Al-5Nb in as-HIPed condition (200 MPa for 2 h at 1250 °C). SEM image taken in BSE mode, i.e.  $\alpha_2$ -Ti<sub>3</sub>Al appears light grey and  $\gamma$ -TiAl grey to dark.

### Texture formation during compressive deformation

In order to analyze the textures formed during near conventional forging, they are compared with textures derived from uniaxial compression tests with the same HIPed Ti-45Al-5Nb starting material. The compression tests were conducted systematically at several temperatures within the ( $\alpha_2$ + $\gamma$ ) phase region each with three different strain rates.<sup>[20]</sup> In this laboratory-scale “forging” experiments cylindrical specimens (10 mm in diameter and 15 mm in height) were deformed to an overall logarithmic strain of approximately 1. After deformation at 700 °C the texture of the  $\gamma$ -TiAl phase shows three orientation maxima when described by inverse pole figures in load direction (Figure 2a). One is formed at  $\langle 110 \rangle$  and a second at about  $\langle 302 \rangle$ . In fcc metals the stable orientations for compressive deformation are  $\langle 110 \rangle$  and  $\langle 101 \rangle$  which are symmetrically equivalent in the cubic system. Due to the tetragonal L1<sub>0</sub> structure of  $\gamma$ -TiAl the ideal cubic maximum at  $\langle 101 \rangle$  is shifted towards  $\langle 100 \rangle$  resulting in  $\langle 302 \rangle$ . A third metastable maximum is formed around  $\langle 411 \rangle$  and is connected with  $\langle 110 \rangle$  and  $\langle 302 \rangle$  by a band showing a high orientation density. Additional computer simulations of the deformation texture have shown that the texture after

compression at 700 °C is exclusively generated by activation of slip systems and mechanical twinning and, therefore, represents a pure deformation texture.<sup>[20]</sup> With increasing deformation temperatures the pure deformation texture diminishes. The metastable maximum vanishes between 800 °C to 900 °C. The maximum around  $\langle 110 \rangle$  becomes continuously weaker and disappears completely at 1100 °C; only the  $\langle 302 \rangle$  deformation texture component stays stable even at this temperature. Simultaneously, at 800 °C the orientation density around  $\langle 100 \rangle$  increases forming a new orientation maximum. Thus, the  $\langle 100 \rangle$  position is the preferred orientation generated during dynamic recrystallization (DRX).<sup>[25]</sup> At 1100 °C the texture is mainly affected by DRX as shown in Figure 2b. The inverse pole figure shows a broad band of orientation density between  $\langle 100 \rangle$  and  $\langle 101 \rangle$ . During DRX new nuclei are generated continuously. Obviously, those nucleated at orientations around  $\langle 100 \rangle$  have the best growing conditions. They grow at the expense of adjoining grains, especially at the expense of grains orientated around  $\langle 110 \rangle$ , which are mainly formed by mechanical twinning. These grains act as starting points for recrystallization<sup>[26]</sup> and are consumed in the course of the recrystallization process. Due to the continuing compressive deformation the new grains formed by DRX rotate towards  $\langle 302 \rangle$ . This process of nucleation, growth and rotation takes continuously place during DRX and provides an obvious explanation for the formation of the orientation band between  $\langle 100 \rangle$  and  $\langle 101 \rangle$  and the vanishing of pure deformation texture components.



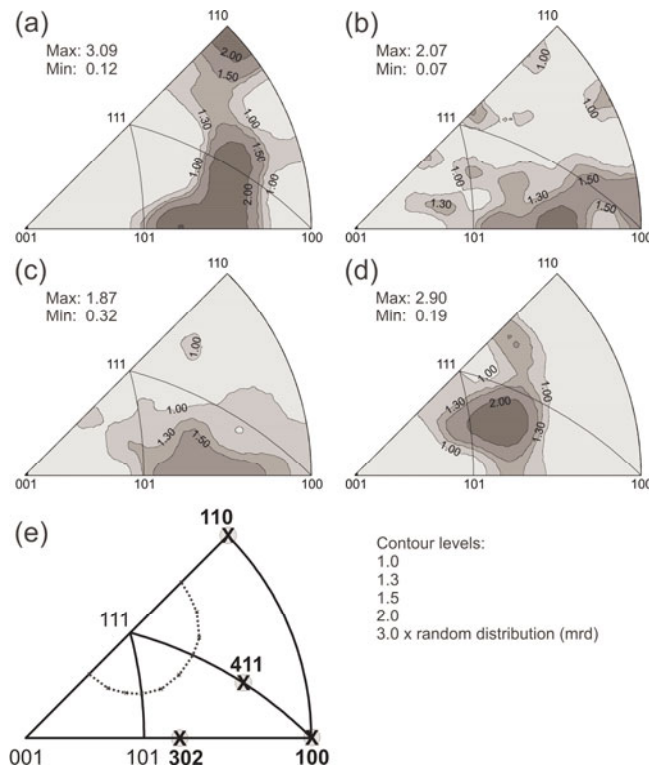


Fig. 2. Texture of the  $\gamma$ -TiAl phase in Ti-45Al-5Nb after compressive deformation. Inverse pole figures in load direction. (a) Pure deformation texture after deformation at 700 °C, (b) DRX texture after deformation at 1100 °C, (c) DRX texture after forging at 1270 °C, and (d) transformation texture after forging close to  $T_{\alpha}$  (~1295 °). (e) Sketch showing the main texture components as discussed in the text; the dotted line represents the 20° distance around  $\langle 111 \rangle$ .

Besides the texture of  $\gamma$ -TiAl the  $\alpha_2$ -Ti<sub>3</sub>Al texture was measured additionally in specimens deformed at temperatures between 800 °C and 1100 °C. The  $\alpha_2$  texture is formed by a tilted  $\langle 0001 \rangle$  basal fiber with a tilt angle between load direction and fiber axis of about 20° (Figure 3a). A typical recalculated  $\{0001\}$  pole figure is shown in Figure 3b. In contrast to the  $\gamma$  texture, the  $\alpha_2$  texture does not change with increasing temperature. Tilted basal fiber textures with a tilt angle of about 20° after compressive deformation are also reported for  $\alpha$ -Ti and other hcp metals with a  $c/a$  ratio  $< 1.63$ .<sup>[27]</sup> That means that during uniaxial compression

at elevated temperatures the same slip systems are activated in  $\alpha_2$ -Ti<sub>3</sub>Al and  $\alpha$ -Ti(Al), making the ordering of  $\alpha_2$ -Ti<sub>3</sub>Al negligible. A crystallographic relationship between the  $\alpha_2$  texture and the  $\gamma$  texture according to the Blackburn relationship  $\{111\}\gamma \parallel \{0001\}\alpha_2$  and  $\langle 1\bar{1}0 \rangle\gamma \parallel \langle 11\bar{2}0 \rangle\alpha_2$  is not observed neither to the  $\gamma$  deformation texture nor to the  $\gamma$  texture formed by DRX. Blackburn related  $\gamma$  texture components of the tilted basal fiber should lay on a ring in 20° distance around the  $\langle 111 \rangle$  orientation in the inverse  $\gamma$  pole figures (in load direction) as shown in Figure 2e. This indicates that the textures of both phases are generated independently of each other during uniaxial compression in the ( $\alpha_2+\gamma$ ) phase field.

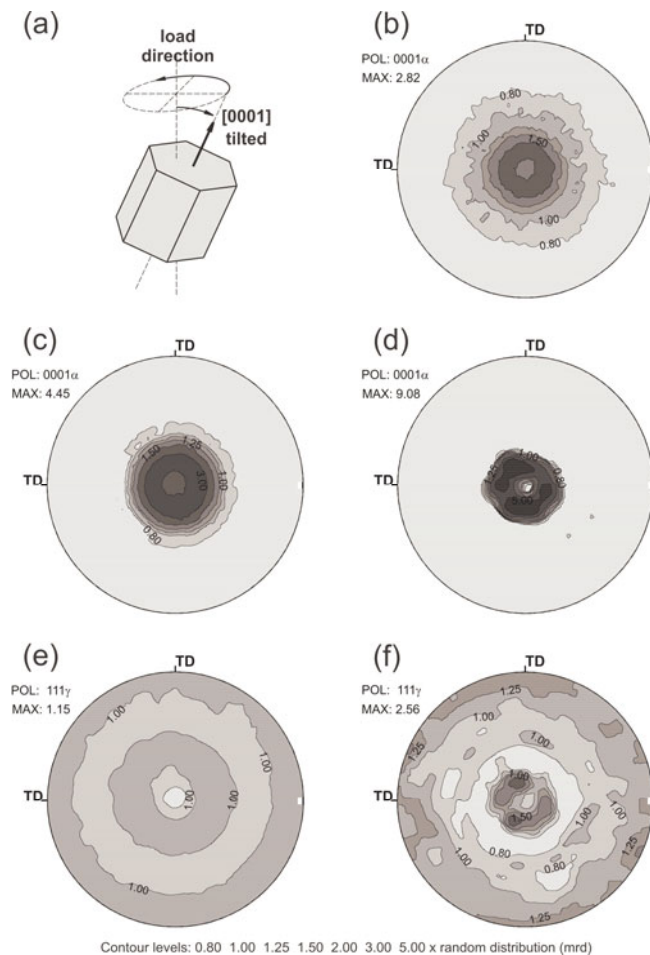


Fig. 3. (a) Orientation of the hexagonal unit cell in a tilted basal fiber texture. (b-f): Recalculated pole figures in load direction after compressive deformation. (b-d):  $\{0001\}\alpha$

pole figures; (b) after deformation at 1100 °C, (c) after forging at 1270 °C and (d) after forging close to  $T_\alpha$ . (e,f): Corresponding  $\{111\}\gamma$  pole figures after forging (e) at 1270 °C and (f) close to  $T_\alpha$ , showing (e) no crystallographic correlation and (f) a strong crystallographic correlation according to the Blackburn relationship.

### Near conventional forging

HIPed powder compacts, fabricated in the same way as used for the compression tests, were forged at Böhler Schmiedetechnik in the  $(\alpha+\gamma)$  phase region at 1200 °C, 1270 °C and close to  $T_\alpha$  ( $\sim 1295$  °) using a hydraulic press without any special isothermal forging equipment.<sup>[11]</sup> The forging experiments were supported by simulation using the finite element simulation software Deform 2D and 3D. From the simulation it was possible to obtain information on temperature, strain, strain rate, and stress distribution during the experiment. This information is essential, because due to the non-isothermal nature of the forging process, all the parameters in the experimental matrix depend on each other (e.g. cooling of billet and die during the process). Thus, when decreasing the die speed to reduce the strain rate during the deformation, the temperature drop in the billet and the dies is more severe and can cause a failure of the forging experiment (appearance of cracks or even breaking of the billet).

The microstructure of the forged samples is shown in Figure 4. The specimen forged at 1200 °C consists of about 75 vol.%  $\gamma$ -TiAl and exhibits a very fine grained microstructure due to a high degree of DRX, see Figure 4a. With increasing forging temperature the  $\gamma$ -TiAl volume fraction decreases<sup>[28]</sup> and the grain size of DRX  $\gamma$ -TiAl rises (Figure 4b). In the specimen forged close to  $T_\alpha$ , see Figure 4c, only a small amount of primary  $\gamma$ -TiAl grains, about 5 vol.%, exists between large former  $\alpha$ -Ti(Al) grains. The former  $\alpha$ -Ti(Al) grains show a distinct aspect ratio. During cooling they transformed to lamellar  $(\alpha_2+\gamma)$  colonies.

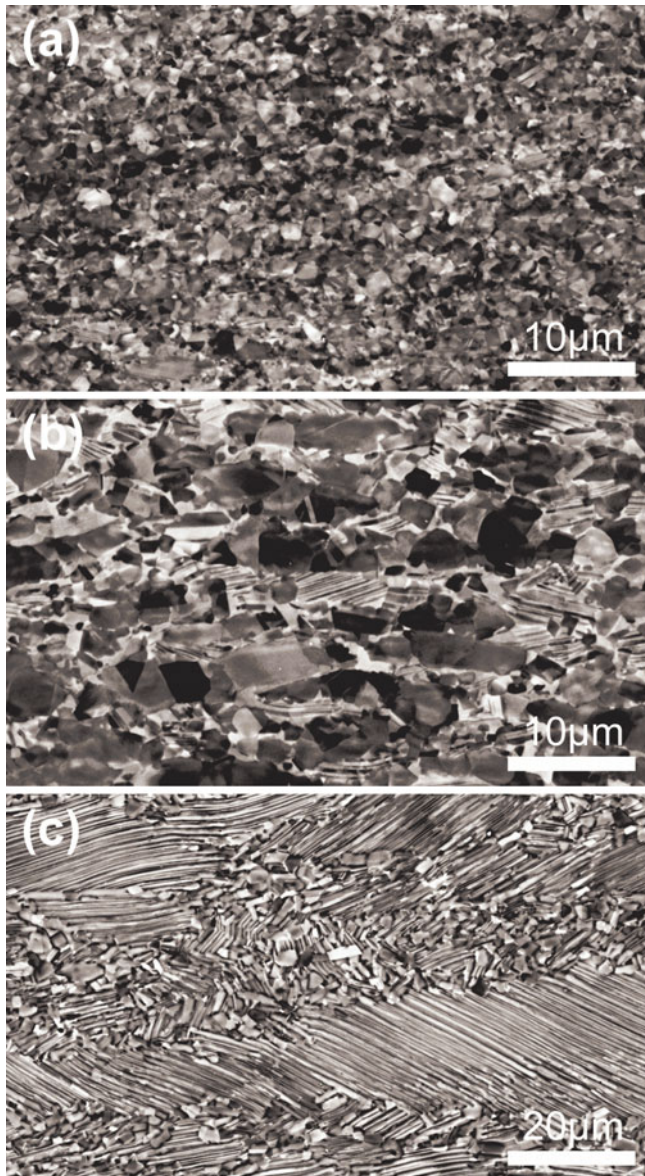


Fig. 4. Microstructure of Ti-45Al-5Nb after forging on an industrial scale at (a) 1200 °C, (b) 1270 °C and (c) close to  $T_{\alpha}$  (~1295 °). SEM images taken in BSE mode, i.e.  $\alpha_2$ -Ti<sub>3</sub>Al appears light grey and  $\gamma$ -TiAl grey to dark. In all images the forging direction is vertical.

The  $\alpha$ -Ti(Al) texture of the forged specimens is formed by a tilted basal fiber similar as it was found after the compression tests, see e.g. Figures 3c,d. With increasing forging temperature the  $\alpha$  texture becomes stronger and sharper because of the almost exclusive

deformation of the  $\alpha$ -Ti(Al) phase at temperatures close to  $T_\alpha$ . Although forging took place at temperatures above the  $\alpha_2$ -Ti<sub>3</sub>Al to  $\alpha$ -TiAl transition no difference is seen when compared to  $\alpha_2$ -Ti<sub>3</sub>Al textures obtained after the compression tests conducted on a laboratory scale within the ( $\alpha_2+\gamma$ ) phase region (Figure 3b). This gives a further argument for the already mentioned activation of the same slip systems in  $\alpha_2$ -Ti<sub>3</sub>Al and  $\alpha$ -Ti(Al) during uniaxial compressive deformation at high temperatures.

After forging at 1200 °C and 1270 °C,  $\gamma$ -TiAl shows a typical DRX texture (Figure 2c) forming a broad orientation band between  $\langle 100 \rangle$  and  $\langle 101 \rangle$ , similar to that present after compression at 1100 °C. This texture is in consistence with the observed DRX microstructure shown in Figures 4a,b. However, the  $\gamma$  texture after forging close to  $T_\alpha$  (Figure 2d) exhibits components that can be explained neither by deformation nor by DRX. It is a distinct transformation texture affected by the transformation of  $\alpha$ -Ti(Al) to  $\gamma$ -TiAl during cooling, whereby the most part of  $\gamma$  has been formed. According to the Blackburn relationship the prior  $\{0001\}\alpha$  orientation is conserved in the  $\{111\}\gamma$  orientation. Thus the main  $\gamma$  texture components lay in a 20° distance around  $\langle 111 \rangle\gamma$  (Figure 2d). Moreover, this correlation is illustrated by the central part of the recalculated pole figures of  $\{0001\}\alpha$  and  $\{111\}\gamma$  (Figures 3d and f). The lower overall orientation density and the additional orientation density at the rim of the recalculated  $\{111\}\gamma$  pole figure is due to the four  $\langle 111 \rangle$  axes of the tetragonal system which are related only to a single  $\langle 0001 \rangle$  axis of the hexagonal system.

## Conclusions

Texture formation was studied in a Ti-45Al-5Nb alloy during near conventional forging on an industrial scale. The textures are compared with those derived from laboratory uniaxial compression tests. Depending on the deformation conditions extreme different  $\gamma$ -TiAl

textures are formed. After deformation at 700 °C the texture of the  $\gamma$ -TiAl phase exhibits pure deformation components. With increasing temperature the texture changes and is predominantly affected by DRX related components at temperatures above 1000 °C. This changing corresponds with microstructural observations. After forging close to  $T_\alpha$  a third  $\gamma$  texture type is formed. It is identified as a transformation texture that shows a significant crystallographic relationship to the former  $\alpha$ -Ti(Al) phase according to the Blackburn relationship. The  $\alpha$ -Ti(Al) and the  $\alpha_2$ -Ti<sub>3</sub>Al phase show a similar texture as it is known for Ti and Ti-alloys after compressive deformation at elevated temperatures. No significant change of the  $\alpha/\alpha_2$  texture is observed in the temperature range between 800 °C and just below  $T_\alpha$ . This indicates that at elevated temperatures the same slip systems are activated in  $\alpha_2$ -Ti<sub>3</sub>Al and  $\alpha$ -Ti(Al), and the additional order of the  $\alpha_2$ -Ti<sub>3</sub>Al structure does not influence the formation of the texture.

## References

- [1] *Structural Aluminides for Elevated Temperature Applications* (Eds: Y.-W. Kim, D. Morris, R. Yang, C. Leyens), TMS, Warrendale, PA, USA, **2008**.
- [2] A. Lasalmonie, *Intermetall.* **2006**, 14, 1123.
- [3] H. Kestler, H. Clemens, in *Titanium and Titanium Alloys* (Eds: C. Leyens, M. Peters), Wiley-VCH, Weinheim, Germany, **2003**, 351.
- [4] F. Appel, M. Oehring, J. D. H. Paul, U. Lorenz, in *Struc. Intermetall.* (Eds: K. Hemker, D. Dimiduk, H. Clemens, R. Darolia, H. Inui, J. Larsen, V. Sikka, M. Thomas, J. Whittenberger), TMS, Warrendale, PA, USA, **2001**, 63.
- [5] S. Bystrzanowski, A. Bartels, H. Clemens, R. Gerling, F.-P. Schimansky, G. Dehm, H. Kestler, *Intermetall.* **2005**, 13, 515.
- [6] V. A. C. Haanappel, H. Clemens, M. F. Stroosnijder, *Intermetall.* **2002**, 10, 293.
- [7] E.A. Loria, *Intermetall.* **2000**, 8, 1339.
- [8] X. Wu, *Intermetall.* **2006**, 14, 1114.
- [9] F. Appel, U. Brossmann, U. Christoph, S. Eggert, P. Janschek, U. Lorenz, J. Müllauer, M. Oehring, J. D. H. Paul, *Adv. Eng. Mater.* **2000**, 2, 699.
- [10] D. Roth-Fagaraseanu, S. Jain, W. Voice, A. Se, P. Janschek, F. Appel, in *Struc. Intermetall.* (Eds: K. Hemker, D. Dimiduk, H. Clemens, R. Darolia, H. Inui, J. Larsen, V. Sikka, M. Thomas, J. Whittenberger), TMS, Warrendale, PA, USA, **2001**, 241.
- [11] S. Kremmer, H. F. Chladil, H. Clemens, A. Otto, in *Ti-2007 Science and Technology, Vol. 2* (Eds: M. Niinomi, S. Akiyama, M. Hagiwari, M. Ikeda, K. Maruyama), The Japan Institute of Technology, Japan, **2008**, 989.
- [12] H. Clemens, W. Wallgram, S. Kremmer, V. Guether, A. Otto, A. Bartels, *Adv. Eng. Mater.* **2008**, 10, 707.
- [13] W. Schillinger, B. Lorenzen, A. Bartels, *Mater. Sci. Eng. A* **2002**, 329-331, 644.

- [14] A. Bartels, W. Schillinger, G. Grassl, H. Clemens, in *Gamma Titanium Aluminides 2003* (Eds: Y.-W. Kim, H. Clemens, A. H. Rosenberger), TMS, Warrendale, PA, USA, **2003**, 275.
- [15] H. Fukotomi, A. Nomoto, Y. Osuga, S. Ikeda, H. Mecking, *Intermetall.* **1996**, 4, 49.
- [16] W. Schillinger, A. Bartels, R. Gerling, H. Clemens, in *Ti-2003: Science and Technology* (Eds: G. Lütjering, J. Albrecht), Wiley-VCH, Weinheim, Germany, **2004**, 2385.
- [17] H. Brokmeier, M. Oehring, U. Lorenz, H. Clemens, F. Appel, *Metallurgical and Materials Transactions A* **2004**, 35, 3563.
- [18] W. Schillinger, A. Bartels, R. Gerling, F.-P. Schimansky, H. Clemens, *Intermetall.* **2006**, 14, 336.
- [19] A. Stark, A. Bartels, R. Gerling, F.-P. Schimansky, H. Clemens, *Adv. Eng. Mater.* **2006**, 8, 1087.
- [20] A. Stark, A. Bartels, F.-P. Schimansky, H. Clemens, in *Advanced Intermetallic-Based Alloys* (Eds: J. Wiezorek, C. L. Fu, M. Takeyama, D. Morris, H. Clemens), MRS Symp. Proc. 980 Warrendale, PA, USA, **2007**, 0980-II07-01.
- [21] R. Gerling, H. Clemens, F.P. Schimansky, *Adv. Eng. Mater.* **2004**, 6, 23.
- [22] M. Dahms, H. J. Bunge, *J. Appl. Crystallogr.* **1989**, 22, 439.
- [23] H. Wenk, S. Matthies, J. Donovan, D. Chateigner, *J. Appl. Crystallogr.* **1998**, 31, 262.
- [24] H.F. Chladil, H. Clemens, H. Leitner, A. Bartels, R. Gerling, F.P. Schimansky, S. Kremmer, *Intermetall.* **2006**, 14, 1194.
- [25] A. Bartels, W. Schillinger, *Intermetall.* **2001**, 9, 883.
- [26] F. Appel, R. Wagner, *Mater. Sci. Eng. R* **1998**, 22, 187.
- [27] *Texturen metallischer Werkstoffe* (Eds: G. Wassermann, J. Grewen), Springer, Berlin, Germany, **1962**, 286.
- [28] L. A. Yeoh, K.-D. Liss, A. Bartels, H.F. Chladil, M. Avdeev, H. Clemens, R. Gerling, T. Buslaps, *Scripta Mat.* **2007**, 57, 1145.



**For the Table of Contents:**

Texture formation was studied in an intermetallic Ti-45at%Al-5at%Nb alloy after uniaxial compression and near conventional forging. Depending on the deformation conditions the texture of the  $\gamma$ -TiAl phase is formed by pure deformation components, components related to dynamic recrystallization, or transformation components. This changing corresponds with microstructural observations. The  $\alpha_2$ -Ti<sub>3</sub>Al and the  $\alpha$ -Ti(Al) phase show a similar texture as it is known for Ti and Ti-base alloys after compressive deformation at elevated temperatures. In contrast to the  $\gamma$  texture, no significant change of the  $\alpha/\alpha_2$  texture was observed in the temperature range between 800 °C and just below the  $\alpha$ -transus temperature ( $T_\alpha = 1295$  °C).

